Development 139, 623 (2012) doi:10.1242/dev.077917

Transmembrane voltage potential controls embryonic eye patterning in *Xenopus laevis*

Vaibhav P. Pai, Sherry Aw, Tal Shomrat, Joan M. Lemire and Michael Levin

There was an error in the version of *Development* **139**, 313-323 published on ePress on December 7th 2011.

The first two authors should have been listed as having contributed equally to this work. The print and final online versions are correct.

The authors apologise to readers for this mistake.

Development 139, 313-323 (2012) doi:10.1242/dev.073759

Transmembrane voltage potential controls embryonic eye patterning in *Xenopus laevis*

Vaibhav P. Pai*, Sherry Aw*,§, Tal Shomrat, Joan M. Lemire and Michael Levin‡

SUMMARY

Uncovering the molecular mechanisms of eye development is crucial for understanding the embryonic morphogenesis of complex structures, as well as for the establishment of novel biomedical approaches to address birth defects and injuries of the visual system. Here, we characterize change in transmembrane voltage potential (V_{mem}) as a novel biophysical signal for eye induction in *Xenopus laevis*. During normal embryogenesis, a striking hyperpolarization demarcates a specific cluster of cells in the anterior neural field. Depolarizing the dorsal lineages in which these cells reside results in malformed eyes. Manipulating V_{mem} of non-eye cells induces well-formed ectopic eyes that are morphologically and histologically similar to endogenous eyes. Remarkably, such ectopic eyes can be induced far outside the anterior neural field. A Ca^{2+} channel-dependent pathway transduces the V_{mem} signal and regulates patterning of eye field transcription factors. These data reveal a new, instructive role for membrane voltage during embryogenesis and demonstrate that V_{mem} is a crucial upstream signal in eye development. Learning to control bioelectric initiators of organogenesis offers significant insight into birth defects that affect the eye and might have significant implications for regenerative approaches to ocular diseases.

KEY WORDS: Membrane potential, Eyes, Bioelectricity, *Xenopus*

INTRODUCTION

Embryonic eye development offers the opportunity to understand the genetic and biophysical mechanisms that drive the self-assembly of complex biological structures (Erclik et al., 2009). Eye tissue formation begins with the regionalization of anterior neural plate into an 'eye field', as evidenced by the expression of eye field transcription factors (EFTFs) (Zaghloul et al., 2005). The eye field is further resolved into bilateral eye primordia by the dynamic expression of EFTFs (Zuber, 2010). However, relatively little is known about the regulation of EFTF bilateral refinement. EFTFs are not induced until neurulation and are not exclusively involved in eye development; Pax6 and Rx1 play important roles in brain development, neuronal migration and other processes. This suggests the existence of as yet uncharacterized additional instructive signal(s) that drive certain embryonic cells specifically toward eye formation. Recent studies identified a cocktail of factors that converts animal cap ectoderm to an eye fate (Viczian et al., 2009; Zuber et al., 2003). Could eyes be induced by an even more minimal set of signals? And, could eye formation be induced in vivo at locations far from the anterior neural field? The identification and characterization of such signals would have tremendous potential for therapeutic applications, as well as shedding light on endogenous mechanisms of lineage restriction and morphogenetic control.

Endogenous steady-state ion currents, voltage gradients and electric fields produced by ion channels and pumps in all cells (not just excitable neurons and muscle) are crucial regulators of patterning (Levin, 2009; McCaig et al., 2009). They control cell migration (McCaig et al., 2009; Prevarskaya et al., 2010; Yao et al., 2008; Yasuda and Adams, 2010), proliferation (Blackiston et al., 2011) and differentiation (Sundelacruz et al., 2009) in a wide variety of systems. Although epithelial electric fields have been implicated in adult eye wound healing (Reid et al., 2005; Wang et al., 2005; Zhao et al., 2006), the roles of ion flows in eye development have not been explored. In *Xenopus laevis*, we have uncovered an endogenous role for plasma membrane voltage gradients during eye development, and show that artificially induced changes in transmembrane potential (V_{mem}) are sufficient to induce well-formed eyes outside of the anterior neural field. Thus, V_{mem} is an important endogenous component of the eye induction cascade and presents a tractable control point for the therapeutic induction of visual system tissues.

Department of Biology and Tufts Center for Regenerative and Developmental Biology, Tufts University, Medford, MA 02155, USA.

*These authors contributed equally to this work
§Present address: Institute of Molecular and Cell Biology, 61 Biopolis Drive, Proteos, Singapore 138673, Singapore
‡Author for correspondence (michael.levin@tufts.edu)

Accepted 3 November 2011

MATERIALS AND METHODS

Animal husbandry and mRNA injection

Xenopus laevis embryos were fertilized in vitro according to standard protocols (Sive et al., 2000) in 0.1× Marc's Modified Ringer's (MMR; 10 mM Na^+, 0.2 mM K^+, 10.5 mM Cl^-, 0.2 mM Ca^{2+}, pH 7.8]. Intracellular ion concentrations in *Xenopus* are: 21 mM Na^+, 90 mM K^+, 60 mM Cl^-, 0.5 mM Ca^{2+} (Gillespie, 1983). *Xenopus* embryos were housed at 14-18°C and staged according to Faber and Nieuwkoop (Faber and Nieuwkoop, 1967). Capped synthetic mRNAs generated using mMessage mMachine (Ambion) were resuspended in water and injected (3 nl per blastomere) into embryos in 3% Ficoll. All experiments were approved by the Tufts University Animal Research Committee in accordance with the Guide for Care and Use of Laboratory Animals.

Imaging of membrane voltage patterns using CC2-DMPE

Fresh CC2-DMPE (Molecular Probes) stocks (1 mg/ml in DMSO) were diluted 1:1000 in 0.1× MMR to 0.2 μM. Embryos were soaked in CC2-DMPE dye for 1.5 hours followed by five washes in 0.1× MMR. Embryos in 0.1× MMR were imaged using 405 nm excitation and 460 nm emission on a Nikon AZ100 microscope with an Andor Luca digital CCD camera and NIS-Elements software.

In situ hybridization

Embryos were fixed in MEMFA [100 mM MOPS (pH 7.4), 2 mM EGTA, 1 mM $MgSO_4$, 3.7% (v/v) formaldehyde] and in situ hybridization was performed as described (Harland, 1991). Probes used were *Otx2* [gift of Dr Valerie Schneider (Pannese et al., 1995)], *Pax6* [gift of Dr Ali Hemmati-Brivanlou (Hirsch and Harris, 1997)] and *Rx1* [gift of Dr Michael Zuber (Andreazzoli et al., 1999)].

Immunofluorescence

Embryos were fixed overnight in MEMFA and stored at 4°C in PBTr (1× PBS, 0.1% Triton X-100), embedded in paraffin and sectioned at 10 μm. Sections were washed three times in PBTr, blocked with 10% goat serum, incubated with primary antibody in PBTr overnight, washed six times with PBTr, and incubated with Alexa Fluor-conjugated secondary antibody (Invitrogen; 1:1000) for 4 hours at room temperature. Sections were then washed, mounted and viewed with an Olympus BX61 spinning-disk confocal microscope with an ORCA digital CCD camera (Hamamatsu) controlled with MetaMorph software. Primary antibodies were: β-crystallin (Abcam ab90379; 1:1000) (Secchi et al., 1976); Glutamine synthetase (Sigma G2781; 1:500) (Pahuja et al., 1985); XAP2 (DSHB clone 5B9; 1:10) (Harris and Messersmith, 1992); Calbindin (Sigma C2724; 1:500) (Gargini et al., 2007); and Islet-1 (DSHB clone 39.4D5; 1:100) (Ericson et al., 1992).

Drug exposure

Stocks of Ivermectin (IVM) (Sigma) were prepared at 10 mM in DMSO. Embryos were exposed in 0.1× MMR to: 10 μM IVM, 0.1 mM Verapamil, 10 μM Fluoxetine or 10 μM Lindane.

Intracellular recordings from embryo cells

Membrane potentials were measured using an oocyte clamp OC-725C amplifier (Warner Instruments, Hamden, CT, USA) with a single voltage electrode. Microelectrodes were made from thin-walled borosilicate glass pulled with a flaming/brown micropipette puller (P-97, Sutter Instruments, Novato, CA, USA) and back filled with electrode solution (2 M potassium acetate, 10 mM KCl, 5 mM HEPES pH 7.5). Tip resistances were 80-100 MΩ. Electrode penetration of ectodermal cells was by visual guidance on a fixed-stage microscope (Zeiss) using a three-axis micromanipulator.

Photoconversion

EosFP mRNA (Gurskaya et al., 2006; Nienhaus et al., 2006; Wacker et al., 2007; Wiedenmann et al., 2004; Wiedenmann and Nienhaus, 2006) was injected into *Xenopus* embryos immediately after fertilization at the one-cell stage. At stage 17/18, the embryos were soaked in CC2-DMPE dye. The CC2-DMPE staining was documented with an Olympus BX61 microscope. The CC2-DMPE-indicated region was exposed to DAPI excitation wavelength using a 40× lens. The photoconversion was documented immediately at stage 17/18 and again at stage 28.

RESULTS

Bilateral hyperpolarized cell clusters appear in the anterior neural field before formation of eye primordia in *Xenopus*

To document real-time changes in V_{mem} during eye development, we used the voltage-sensitive dye CC2-DMPE (Wolff et al., 2003) to detect hyperpolarization in the *Xenopus* embryo in vivo. A physiological screen for bioelectric patterns during craniofacial development (Vandenberg et al., 2011) revealed that, starting at stage 17/18, normal embryos exhibit two small areas in the anterior neural field that are bilaterally positioned and hyperpolarized relative to their neighbors (Fig. 1A, red arrowheads). Whole-cell electrophysiological recordings of V_{mem} from these areas and from the neighboring tissues on the flank of the same embryo (Fig. 1B) revealed that the CC2-DMPE-demarcated domains were hyperpolarized relative to neighboring tissues by ~10 mV (also confirming the ability of the CC2-DMPE dye to detect cells with hyperpolarized V_{mem}). Other regions of the embryo also exhibit

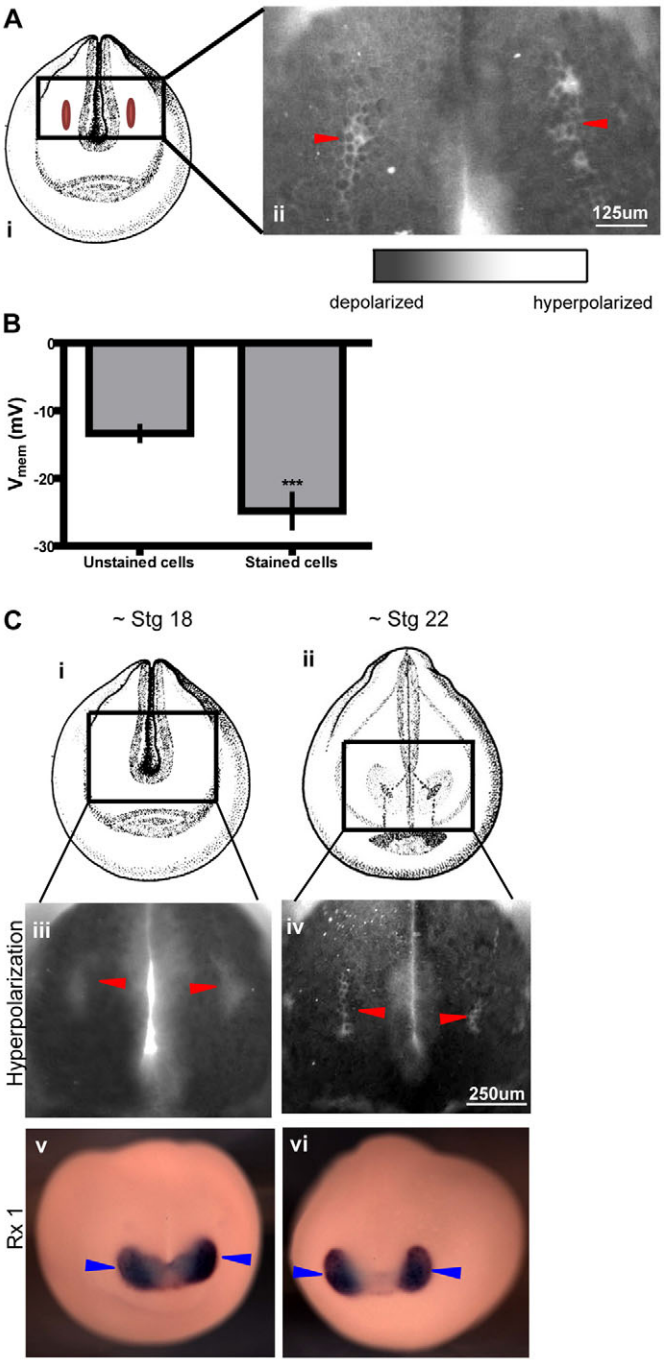

Fig. 1. A bilateral cluster of hyperpolarized cells appears in the anterior neural field before the formation of eye primordia. (**A**) CC2-DMPE staining (ii) showing the relative V_{mem} of cells in the indicated region (i) of a stage 18 *Xenopus* embryo. Arrowheads indicate the specific clusters of hyperpolarized cells in the anterior neural field. (**B**) Electrophysiological V_{mem} measurements of cells identified by CC2-DMPE staining versus their neighboring unstained cells. Readings were recorded from at least six embryos. Values are mean ± s.e.m. ***, P=0.0002. (**C**) CC2-DMPE staining (iii,iv) and, immediately thereafter, *Rx1* in situ hybridization (v,vi) of the indicated regions (i,ii) of *Xenopus* embryos at stages 18 and 22. Red arrowheads mark specific clusters of hyperpolarized cells in the anterior neural field. Blue arrowheads indicate *Rx1* expression in the same embryos. The bilateral hyperpolarization signal occurs before the formation of bilateral eye primordia. See also supplementary material Fig. S1, Table S1. Illustrations reproduced with permission from Nieuwkoop and Faber (Nieuwkoop and Faber, 1967).

interesting distributions of V_{mem}; these are described elsewhere (Vandenberg et al., 2011) and will be investigated in subsequent work.

V_{mem} collapses upon cell death and thus cannot be imaged simultaneously with in situ hybridization. We imaged the hyperpolarized V_{mem} signal using CC2-DMPE at stage 17/18 and immediately fixed the embryos for in situ hybridization analysis of the EFTFs *Otx2*, *Rx1* and *Pax6* (Fig. 1C; data not shown). The relatively broad anterior expression of EFTFs appeared to overlap with the hyperpolarized cells (Fig. 1C; data not shown).

To overcome the incompatibility of in situ hybridization with in vivo physiological imaging and to more precisely characterize the timing and co-localization of the observed hyperpolarized cell cluster in relation to the formation of eye primordia, we verified the overlap by labeling the CC2-DMPE-demarcated hyperpolarized cells using a photoconvertible protein (Wacker et al., 2007). Fertilized eggs were injected with *EosFP* (a green fluorescent protein) mRNA and, at stage 18, as small an area as possible centered on the hyperpolarized cells was photoconverted. Observation of the resulting red signal at stage 28 confirmed that the hyperpolarized cells indeed contribute to eye formation (supplementary material Fig. S1A-C). Agarose sectioning of the embryo through the eye showed that the photoconverted cells contribute to both the lens and the retinal layers of the eye (supplementary material Fig. S1D-F). The hyperpolarized area pattern remains bilateral and largely unchanged through anterior development (stage 22; Fig. 1C; supplementary material Table S1). By contrast, the EFTFs undergo a bilateral regionalization by stage 22, as expected (Fig. 1C) (Viczian et al., 2009; Zuber et al., 2003). The distinct bioelectrical regionalization of the anterior neural field suggests that the bilateral hyperpolarized areas might be involved in the processes by which dynamic expression of the EFTFs regulates the formation of eyes.

Local perturbation of V_{mem} causes disruption of normal eye development

To determine whether hyperpolarization is functionally required for eye development, we performed a loss-of-function experiment by depolarizing V_{mem} of the relevant cells. We used the constitutively conductive EXP1 cation channel (Beg and Jorgensen, 2003) and the glycine-gated chloride channel (GlyR) (Davies et al., 2003), which can be permanently activated by the specific GlyR opener Ivermectin (IVM) (Shan et al., 2001). The use of two different molecular reagents (channels that share no sequence or structural homology and have in common only their effect on membrane potential) specifically tested the role of V_{mem} per se, independent of possible other functions of a particular channel protein or ion species.

In standard 0.1× MMR medium, these channels work to depolarize cells (supplementary material Fig. S2A) (Beg and Jorgensen, 2003; Blackiston et al., 2011; Davies et al., 2003). Embryos were injected with *GlyR* or *EXP1* mRNA in the dorsal two cells of the four-cell embryo [the blastomeres from which eyes derive (Moody, 1987)] (supplementary material Fig. S2Ai) and were stained with CC2-DMPE dye at stage 19 (supplementary material Fig. S2Aii). *GlyR*-injected embryos were treated with the channel opener IVM from stage 17 to 23 to enable the efflux of chloride that depolarizes GlyR-expressing cells. In contrast to uninjected embryos, which show distinct bilaterally hyperpolarized cell clusters (supplementary material Fig. S2Aiii, green arrowheads), *GlyR* and *EXP1* misexpression strongly reduced or disrupted the hyperpolarization pattern in the injected embryos (supplementary material Fig. S2Aiv). This confirmed that our reagents produce the expected loss-of-function effect on the hyperpolarization pattern. We saw no signs of general toxicity or ill-health from ion channel mRNAs, which were titrated to the lowest levels needed to produce eye phenotypes: dorsoanterior index, midline patterning, overall growth rate and proportion, and behavior were all normal, ruling out simple toxicity as a cause of eye malformation. Consistent with existing evidence of V_{mem} changes being associated with specific tissue outcomes (Blackiston et al., 2011; Levin et al., 2002; Levin, 2009; Sundelacruz et al., 2009; Tseng et al., 2010), we occasionally observed additional interesting patterning phenotypes involving other organs, which will be characterized in subsequent studies.

To determine whether the observed hyperpolarization is required for normal eye development, *GlyR* or *EXP1* mRNA was injected into the dorsal blastomeres at the four-cell stage and the embryos scored for eye development at stage 42 (Fig. 2A). Uninjected, *lacZ*-injected, *GlyR*-injected and IVM-treated embryos served as controls. Control embryos had intact, fully closed, well-formed eyes (Fig. 2B). By contrast, expression of *GlyR* plus IVM treatment, or expression of *EXP1* mRNA, caused a high incidence of disrupted endogenous eye formation (48% and 46%, respectively; Fig. 2A). Phenotypes included incomplete eye formation (supplementary material Fig. S2Bi), small (supplementary material Fig. S2Bii) or absent (Fig. 2B) eyes, fusion to the brain (supplementary material Fig. S2Biii) and pigmented optic nerves (supplementary material Fig. S2Biv).

Although bioelectric events can exert effects at long range (Blackiston et al., 2011; Morokuma et al., 2008), the position of the bilateral hyperpolarized regions suggested a local role. We examined the effects of inducing depolarization elsewhere in the embryo. Injection of *GlyR* mRNA plus IVM treatment or of *EXP1* mRNA into the two ventral blastomeres (which make a minor contribution, if any, to eye fate lineages) caused no significant effect on eye development (Fig. 2A). To allow a direct comparison of the injected and uninjected sides of the same embryo and to further test the effective range of influence of hyperpolarization, only one side (one dorsal cell at the four-cell stage) of the embryo was targeted by depolarizing channel mRNA (*GlyR* plus IVM, Fig. 2B; *EXP1*, supplementary material Fig. S2Biii) while leaving the contralateral side as an internal control. The mRNA was mixed with a lineage tracer (*lacZ* mRNA); eye defects occurred only in regions that had been targeted by the depolarizing mRNA, whereas normal eye development occurred on the uninjected region of the same embryo (Fig. 2B; supplementary material Fig. S2Biii). Taken together, these results demonstrate that the bilateral hyperpolarized cell clusters in the anterior neural field are an important, specific component of normal eye development and that this signal works in a local fashion.

To confirm the role of specific V_{mem} levels in eye induction, we took advantage of the ability to control the V_{mem} of GlyR-expressing cells (plus IVM) by modulating the extracellular chloride content $[Cl^-]_{ex}$. The depolarizing effect of *GlyR* misexpression can be progressively reduced by increasing $[Cl^-]_{ex}$ toward the intracellular chloride concentration (Blackiston et al., 2011; Davies et al., 2003), at which point chloride efflux (and depolarization) will cease. After *GlyR* mRNA injection into the dorsal two cells at the four-cell stage, we incubated the embryos (with IVM) at different levels of $[Cl^-]_{ex}$ (stage 17-23). A progressive decrease in the incidence of the malformed eye phenotype (from 48% to 21% at stage 42) was seen as $[Cl^-]_{ex}$ was

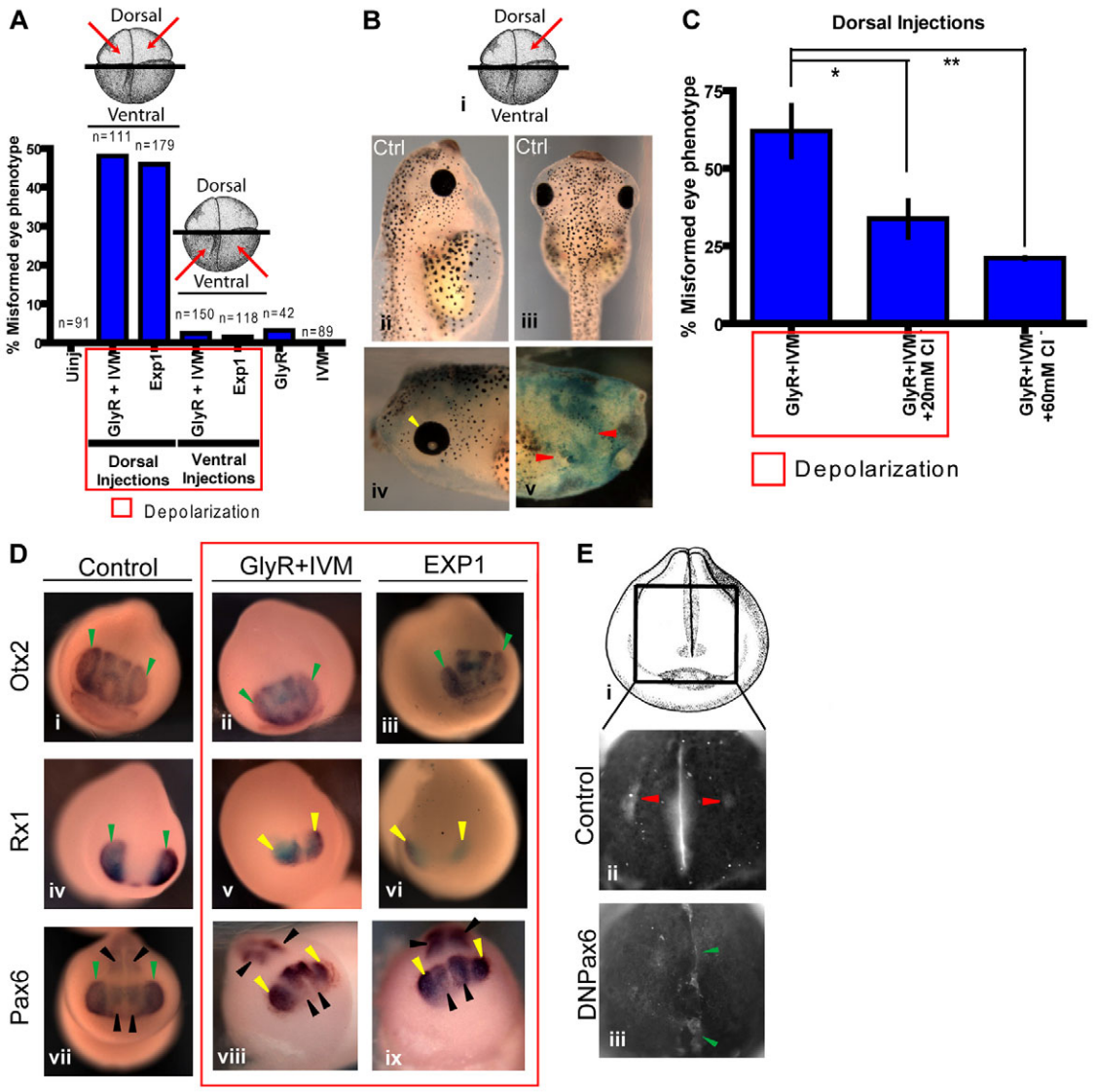

Fig. 2. Local perturbation of V_{mem} disrupts endogenous eye development. (**A**) Quantification of tadpoles with eye phenotypes upon microinjection of *EXP1* or *GlyR* (± IVM treatment) ion channel mRNA in the dorsal or ventral two cells (red arrows) of the four-cell *Xenopus* embryo. A high incidence of malformed eyes is observed in dorsal injections in comparison to controls or ventral injections. (**B**) (i) Four-cell *Xenopus* embryos were injected (red arrow indicates injected cell). (ii,iii) Stage 42 control (uninjected) tadpoles. (iv,v) Stage 42 tadpoles injected with *GlyR* mRNA plus IVM treatment. *lacZ* lineage tracer mRNA was co-injected with the ion channel mRNA. Yellow arrowhead indicates normal eye in the absence of β-gal (blue-green), whereas the red arrowhead indicates an absent eye on the contralateral side of the same tadpole in the presence of β-gal. (**C**) Quantification of tadpoles with malformed eyes at stage 42 after microinjecting *GlyR* plus IVM treatment in two dorsal cells at the four-cell stage and incubation in different concentrations of choline chloride (0, 20 and 60 mM). 60 mM is the isomolar concentration. A depolarization dose-dependent decrease in malformed eye incidence is observed. Values are mean ± s.e.m. (n=3). *, P<0.05; **, P<0.01; one-way ANOVA with Tukey's post test. (**D**) Stage 22 control (uninjected) embryos (i,iv,vii) and embryos microinjected with *GlyR* mRNA plus IVM treatment (ii,v,viii) or *EXP1* mRNA (iii,vi,ix) in the two dorsal cells at the four-cell stage. In situ hybridization for *Otx2* (i-iii), *Rx1* (iv-vi) and *Pax6* (vii-ix) shows a significantly disrupted expression (yellow arrowheads) of *Rx1* [GlyR+IVM, 53% disrupted (n=15); EXP1, 50% disrupted (n=18)] and *Pax6* [GlyR+IVM, 56% disrupted (n=9); EXP1, 57% disrupted (n=7)], whereas *Otx2* expression remains unchanged (green arrowheads) [GlyR+IVM, 92% normal (n=26); EXP1, 94% normal (n=17)]. The black arrowheads indicate *Pax6* expression in the forebrain and the spinal cord, which remain largely unchanged. (**E**) CC2-DMPE staining showing the relative V_{mem} of cells of the indicated region (i) in the stage 19 *Xenopus* embryo. Red arrowheads mark the specific bilateral cluster of hyperpolarized cells in the anterior neural field of control (uninjected) embryos (ii). Green arrowheads mark the disrupted hyperpolarization pattern in embryos microinjected with dominant-negative *Pax6* in the dorsal two cells at the four-cell stage (iii); 76% (n=25) of dominant-negative *Pax6*-injected embryos showed a disrupted CC2-DMPE staining pattern. See also supplementary material Fig. S2. Illustrations reproduced with permission from Nieuwkoop and Faber (Nieuwkoop and Faber, 1967).

increased toward isomolar (60 mM) levels, which abolished the normal outward gradient for these negative charges (Fig. 2C, red box). The ability to rescue the phenotype and control eye patterning by modulating $[Cl^-]_{ex}$, in a dose-responsive manner in accordance with the predictions of the Goldman equation, points to the importance of specific V_{mem} levels in eye development. We could not achieve 100% penetrant rescue, as the levels of $[Cl^-]_{ex}$ could not be raised to higher values without perturbing other voltage-

sensitive systems during patterning that might act as confounding factors (Blackiston et al., 2011; Levin et al., 2002; Levin, 2009; Sundelacruz et al., 2009).

Perturbation of V_{mem} during early development disrupts expression patterns of eye development markers

The bilateral hyperpolarization of cell clusters precedes the bilateral regionalization of the EFTFs (*Rx1* and *Pax6*) (Fig. 1) and this V_{mem} signal is important for proper eye development (Fig. 2). But where does the hyperpolarization V_{mem} signal function within the hierarchy of known signals, such as *Otx2*, *Rx1* and *Pax6*? We analyzed the expression of these genes in V_{mem}-perturbed embryos. Embryos were injected in the dorsal two cells at the four-cell stage with depolarizing mRNAs (*GlyR* or *EXP1*) and fixed at stage 22. *Otx2*, *Rx1* and *Pax6* mRNA expression was detected using antisense mRNA probes (Fig. 2D). *Otx2* is a marker for anterior neural plate (Acampora et al., 1995) and *Pax6* and *Rx1* are highly expressed in the eye field and in certain regions of the central nervous system, including the hypothalamus and the pineal gland (Bailey et al., 2004; Gehring and Ikeo, 1999). The expression pattern of *Otx2* remained unchanged by depolarization (Fig. 2D, green arrowheads), suggesting that overall anterior neural/brain development [which provides crucial signals for eye induction (Lupo et al., 2002)] is not affected by the depolarization. This was confirmed by the observation that there was no change in the robust midline expression of sonic hedgehog (*Shh*) in treated embryos (supplementary material Fig. S2D), nor in the non-eye neural expression of *Pax6* (Fig. 2D, black arrowheads). By contrast, expression of the EFTFs *Rx1* and *Pax6* within the eye domains was significantly reduced (in area, not expression intensity) or mispatterned in embryos in which the V_{mem} of hyperpolarized cell clusters had been artificially depolarized (Fig. 2D, yellow arrowheads). These results suggest that this bioelectrical signal functions to regulate the bilateral patterning of *Pax6* and *Rx1*, confirming the functional importance of V_{mem} for the normal events of eye induction.

Feedback loops and cross-talk between biophysical and genetic pathways are common in patterning systems (Huang and Ingber, 2006; Ingber, 2006; Levin, 2006; Levin, 2009). We asked whether EFTFs could in turn affect the V_{mem} of the hyperpolarized cell clusters. Microinjection of mRNA encoding a dominant-negative mutant of Pax6 (DNPax6) resulted in embryos that lack eyes or have small eyes (Chow et al., 1999) (supplementary material Fig. S2C). We incubated the uninjected and DNPax6-injected embryos in CC2-DMPE dye to monitor the hyperpolarization signal. Interestingly, reduction in *Pax6* activity caused a loss of the hyperpolarization signal in the anterior neural field (Fig. 2E), suggesting the presence of a positive-feedback loop between the hyperpolarization signal and *Pax6* expression in the presumptive eye field cell cluster.

Perturbation of V_{mem} is sufficient to induce ectopic eyes outside the anterior neural field

Having shown that a specific bioelectrical state is necessary for normal eye development, we next asked whether modulation of V_{mem} outside of the normal eye field could be sufficient to induce ectopic eyes. The V_{mem} of cells is determined by the combined activity of numerous endogenously expressed channels and pumps. Extensive expression profiling and quantitative physiological modeling would be required for a comprehensive understanding of the natively expressed conductances that give rise to distinct V_{mem} signals within the *Xenopus* face. Our interest was in probing a range of non-eye regions for their capacity to form eyes and in developing a gain-of-function technology that might be useful in regenerative applications without requiring a complete physiomic analysis. Hence, we targeted a widely expressed ion translocator.

The ATP-sensitive potassium channel (K_{ATP}) is a biomedically important ion channel that is involved in linking V_{mem} to cellular functions in many systems (Nichols, 2006). All four subunits of the K_{ATP} channel (Kir6.1, Kir6.2, SUR1 and SUR2) were found to be expressed in the head region (including the eye fields) and along the dorsal trunk regions of the embryo from early development (stage 15/16) to tail bud stages (data not shown). We used two well-characterized dominant-negative constructs targeting Kir6.1: either the Kir6.1 pore mutant (DNKir6.1p) or the endoplasmic reticulum (ER)-retention mutant (DNKir6.1-ER) (Ficker et al., 2000; Schwappach et al., 2000).

To verify the effect of DNKir6.1p constructs on the V_{mem} of injected cells, we injected the mRNAs into the dorsal two cells of four-cell embryos and then imaged them using the CC2-DMPE dye. Control (uninjected) embryos showed the characteristic hyperpolarization pattern (supplementary material Fig. S3A). DNKir6.1p-injected embryos showed highly diminished, or an absence of, hyperpolarized cell clusters (supplementary material Fig. S3A), confirming the ability of DNKir6.1p to depolarize cells.

mRNAs encoding these dominant-negative K_{ATP} constructs were injected into all four blastomeres of four-cell embryos. The embryos were scored for eye phenotype at stage 42. Green fluorescent protein (*GFP*) and *lacZ* mRNA negative-control injections did not produce any eye-relevant phenotypes (Fig. 3A-C). By contrast, DNKir6.1p and DNKir6.1-ER injections resulted in a high incidence (45% and 35%, respectively) of eye-related phenotypes (Fig. 3A). Approximately 25% of injected embryos had defects in their endogenous eyes, as expected when dorsal cell V_{mem} is perturbed (Fig. 3A,D). Strikingly, ~20% of the embryos exhibited ectopic eye tissue (only lens or only pigmented epithelium), including patches of retinal pigmented epithelium (RPE) (Fig. 3E, red arrowheads) and lens tissue (Fig. 3I,J, blue arrowheads). We also observed embryos (7.5%) with ectopic and well-formed large complete eyes (RPE, retina and lens) (Fig. 3F-H, red arrowheads). Remarkably, ectopic eyes were found not only in the head but also on the gut (Fig. 3G, red arrowhead) and other caudal areas (Fig. 3H, red arrowheads). Ectopic lens tissue, revealed by β-crystallin antibody, occurred in the head region (Fig. 3J, inset) and even the tail (Fig. 3I, blue arrowheads), with islands of ectopic lens tissue found on both the ventral and dorsal side of the embryo (Fig. 3J, blue arrowheads). Although the majority of the ectopic tissues formed in the head (supplementary material Fig. S3B), a unique aspect of this phenotype is that eye components were frequently observed in locales well outside the anterior neural field, including the distal tail (Fig. 3H-J) and the lateral plate mesoderm (Fig. 3L). This was not accompanied by any axial or anterior duplication.

Our results suggest that perturbation of V_{mem} is sufficient to induce an eye fate even in regions that are outside of the normal fate map of tissues competent to become eyes (Zaghloul et al., 2005). Moreover, a single mRNA encoding a bioelectric target is sufficient to kick-start the entire eye development process in distal tissues.

To ensure that the key instructive signal was indeed carried by V_{mem} per se, and not by an ion-specific or ion-independent (e.g. scaffolding) role of our channel constructs, we tested several different ion channels that share no sequence or structural homology but do control V_{mem}. A majority of these induced ectopic

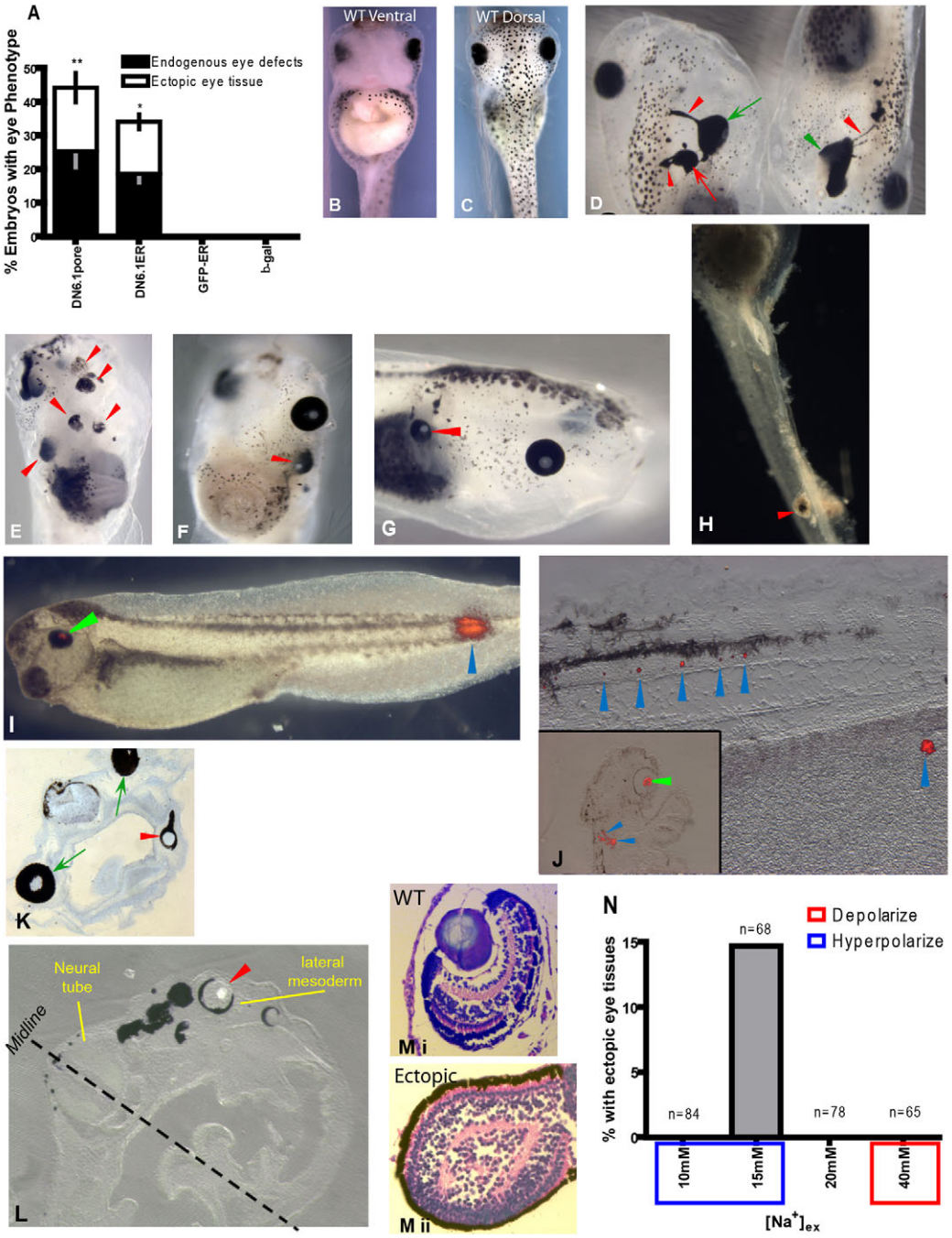

Fig. 3. Dominant-negative K_{ATP} channel subunits cause defects in endogenous eye development and induce a variety of ectopic eye tissues. (**A**) Stage 42 tadpoles showed a significantly high incidence of eye phenotypes (both malformed eyes and ectopic eye tissue) upon microinjection of dominant-negative K_{ATP} mRNAs (DNKir6.1p and DNKir6.1-ER), in comparison to control injections, in all four cells of four-cell embryos. Values are mean ± s.e.m. (n=5). *, P<0.05; **, P<0.01; one-way ANOVA, Tukey's post test. (**B-H**) Stage 42 control tadpoles (B,C) and those microinjected with DNKir6.1p mRNA (D-H) as detailed in A. Green arrow and arrowhead mark endogenous eyes. Red arrow and arrowheads mark ectopic eye tissues. E shows multiple ectopic patches of RPE. Note whole ectopic eyes with lens (F,G) and ectopic eye tissue in tail (H). (**I**,**J**) β-crystallin immunostaining (red) in stage 42 whole tadpole (I) and lateral sections through tadpoles (J) injected with DNKir6.1p mRNA in all four cells at the four-cell stage. Blue arrowheads mark distinct ectopic lens tissue in head and tail region, with green arrowheads marking the endogenous eye lens tissue. (**K**,**L**) Transverse sections of stage 42 tadpoles microinjected with DNKir6.1p mRNA in all four cells at the four-cell stage. Green arrows marks endogenous eyes and red arrowheads mark ectopic eye tissues. Note that the ectopic eye is present on the ventral side of the tadpole in K and along lateral mesoderm in L. (**M**) Hematoxylin and Eosin staining of the endogenous eye (i) and ectopic eye tissue (ii) show a similar histological organization of cell layers. (**N**) A narrow range of membrane voltage induces ectopic eye tissue. Quantification of tadpoles with ectopic eye tissues at stage 42 upon microinjection of neonatal *Nav1.5* channel mRNA in all four cells at the four-cell stage. To vary the V_{mem} in injected cells by control of influx of positive ions through this channel, embryos were incubated in different concentrations of sodium gluconate (10, 15, 20 and 40 mM); 20 mM is isomolar with intracellular sodium (equilibrium). Ectopic eyes were induced only in the hyperpolarizing condition created by 15 mM sodium gluconate. See also supplementary material Fig. S3, Table S2.

eyes, as predicted (supplementary material Table S2). We also asked whether the eye phenotype (ectopic eyes and disrupted endogenous eyes) induced by the depolarizing DNKir6.1p channel could be rescued by co-injection of hyperpolarizing Kv1.5 channel. Among the embryos co-injected with Kv1.5 and DNKir6.1p, only 2% had ectopic eyes and 11% had disrupted eyes, in comparison to 20% and 25%, respectively, in embryos injected with only DNKir6.1p. The rescue of phenotype by a genetically unrelated but physiologically counteractive protein demonstrates the importance of V_{mem} itself as a regulatory factor in the modulation of eye development.

Further, we analyzed whether a narrow V_{mem} range is required for eye formation. We injected embryos with mRNA encoding a sodium channel, Nav1.5, and incubated them in medium containing a range of $[Na^+]_{ex}$, thus generating conditions ranging from hyperpolarizing to depolarizing (as predicted by the Goldman equation). Maximum ectopic eye induction was observed within a small range of hyperpolarizing $[Na^+]_{ex}$ (Fig. 3N), confirming specific V_{mem} values as the information-bearing signal. Taken together, these results support the hypothesis that regulation of V_{mem} per se is an instructive signal in initiating eye induction.

We then performed experiments to determine whether ectopic eye induction involves: (1) the 'migration' of endogenous eye fate cells to ectopic locations upon perturbation of their V_{mem}; (2) the 'colonization' of ectopically injected tissues (perturbed V_{mem}) by attracting endogenous eye fate cells; or (3) the induction of non-eye fate cells to take on eye fate upon perturbation of their V_{mem}. We injected DNKir6.1p (with *lacZ* mRNA as a lineage label) into the dorsal and ventral blastomeres at the four-cell stage. There was no statistical difference between the incidence of ectopic eyes in dorsal (16%) versus ventral (20%) injections (data not shown). Further, whole-mount staining and sections through the ectopic eye tissue at stage 43 showed that all of the ectopic eye tissues were β-gal-positive (supplementary material Fig. S3Biii; data not shown). These results suggest that ectopic eye tissues are induced in a local manner by inducing the injected non-eye fate cells to assume eye identity and not by the migration of, or colonization by, endogenous eye-fated cells.

Bioelectrically induced eyes exhibit morphology and tissue organization similar to endogenous eyes

We next characterized in detail the ectopic eyes induced by V_{mem} change, to determine how closely the ectopic structures resemble normal eyes. Sectioning at stage 46 revealed that the ectopic tissues (Fig. 3K,L, red arrowheads) have a cup-shaped architecture similar to that of endogenous eyes (Fig. 3K,L, green arrows). Histological staining with Hematoxylin and Eosin showed that the ectopic cells (Fig. 3Mii) are organized in morphological layers similar to those of wild-type endogenous eyes (Fig. 3Mi).

We were able to identify and localize the key retinal cell populations in endogenous and ectopic eye tissues by immunostaining: Muller glia (Glutamine synthetase, red), amacrine cells (Islet-1, cyan), rods (XAP2, yellow) and cones (Calbindin, green) (Fig. 4A). A functional retina requires a precise arrangement of retinal cell layers. Co-immunolocalization showed that, in the ectopic eye tissue (Fig. 4B), the Muller glia, amacrine cells, rods and RPE are arranged almost identically to those in wild-type or endogenous eyes (Fig. 4B). Our histological and immunohistochemical analysis showed that bioelectric induction can give rise to most tissues present in the mature eye. Moreover, the ectopic structures formed by perturbation of V_{mem} contain the same tissues, in a similar arrangement, as endogenous eyes.

Formation of ectopic eye tissues by perturbation of V_{mem} involves ectopic induction of eye marker genes

Pax6 has been shown to induce ectopic eyes in *Xenopus* embryos upon overexpression (Chow et al., 1999; Zuber et al., 2003). Does V_{mem} modulation induce eyes through the same EFTFs that are involved in primary (endogenous) eye development? Embryos were injected with DNKir6.1p mRNA, fixed at stage 30, and expression of the anterior neural marker *Otx2* and of the EFTFs *Rx1* and *Pax6* detected by in situ hybridization.

DNKir6.1p injections (which produce ectopic eyes) did not induce ectopic expression of *Otx2*; by contrast, injected embryos showed numerous foci of ectopic *Pax6* and *Rx1* expression well away from the head (Fig. 4C). Thus, bioelectric induction of ectopic eye tissue involves the upregulation of key EFTFs. These data also demonstrate that V_{mem} changes are able to induce de novo expression of EFTFs (Fig. 4C), in addition to regulating their bilateral patterning (Fig. 1, Fig. 2D).

V_{mem} changes are transduced by Ca^{2+} influx during ectopic eye induction

To determine how V_{mem} changes are transduced into effector cascades during eye development, we injected *Kv1.5* mRNA into two cells of four-cell embryos to induce ectopic eye tissue and performed a simple suppression screen (Table 1), blocking a range of targets known to mediate the linkage between bioelectric and transcriptional pathways in other systems (Levin, 2007). Blockade of gap junction-mediated or serotonergic (Fukumoto et al., 2005) signaling did not prevent ectopic eye tissue induction. By contrast, blockade of voltage-gated Ca^{2+} channels (VGCCs) (100 μM Verapamil), significantly reduced the ectopic eye tissue induction by ion channel misexpression. Hence, changes of V_{mem} that induce ectopic eye tissues are likely to be transduced into downstream cascades by VGCC-mediated Ca^{2+} influx – a common mechanism for coupling electrical signaling to changes in cell behavior (Nakanishi and Okazawa, 2006; Nishiyama et al., 2008).

DISCUSSION

Morphogenetic roles for V_{mem} have been demonstrated in egg-oocyte systems (Woodruff and Telfer, 1980), appendage regeneration (Adams et al., 2007) and axial patterning (Beane et al., 2011; Kurtz, and Schrank, 1955; Marsh and Beams, 1947; Shi and Borgens, 1995) in a wide variety of species (Levin, 2009; McCaig et al., 2009). Having screened for bioelectrical pre-pattern during the development of *Xenopus* embryos (Vandenberg et al., 2011), we observed a bilateral, distinctly hyperpolarized cluster of cells in the anterior neural field and show that this hyperpolarization is required for normal eye development.

Eye defects were induced by two independent means of depolarizing anterior neural field cells: misexpression of a depolarizing cation channel (EXP1) or of a chloride channel (GlyR). In the latter case, modulation of $[Cl^-]_{ex}$ allowed control of the magnitude of the effect (in accordance with the Goldman equation) (Blackiston et al., 2011). The ability to disrupt eye development using distinct constructs that mediate the flux of different ions (sodium, potassium or chloride) and have in common only their effect on V_{mem} strongly supports the V_{mem} signal as a factor necessary for normal eye development.

Molecular analysis revealed that perturbing the endogenous V_{mem} signal altered the endogenous expression pattern of *Rx1* and *Pax6*. Additionally, manipulating the V_{mem} of non-eye cells induces de novo *Rx1* and *Pax6* expression. These results suggest

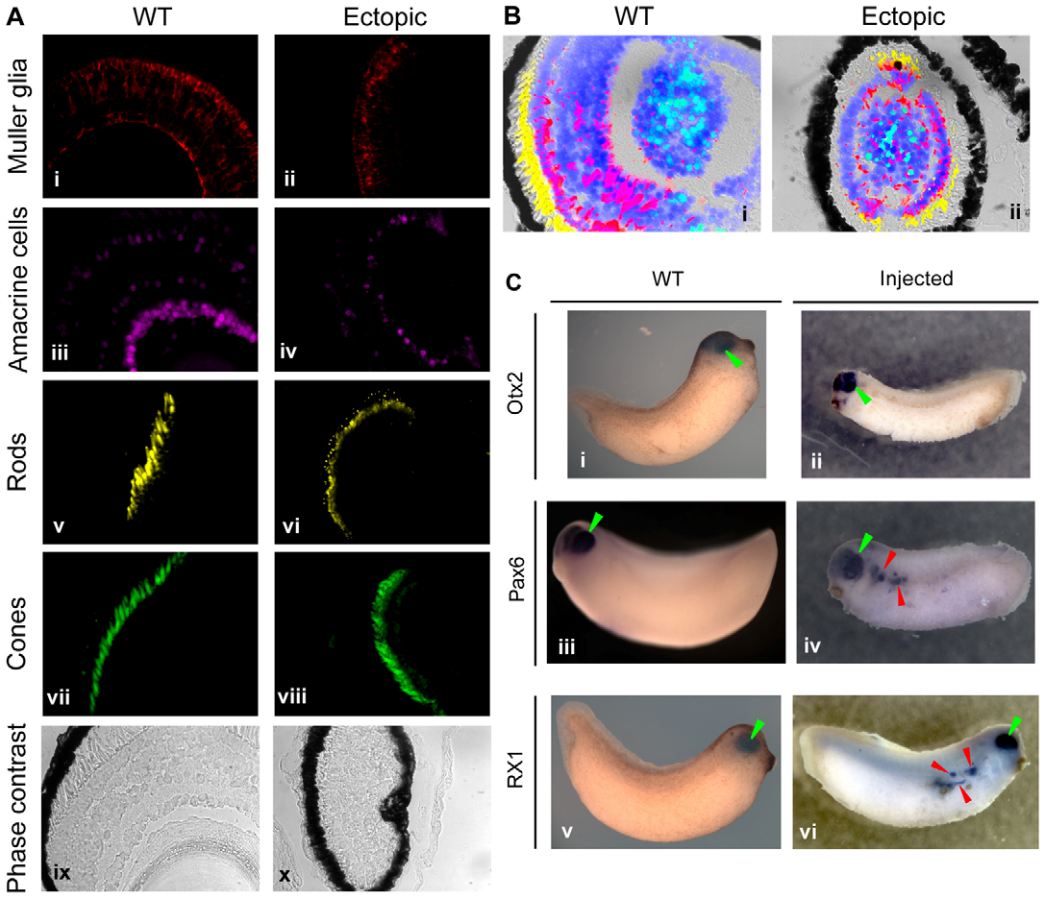

Fig. 4. Ectopic eyes induced by V_{mem} signal are similar to endogenous eyes and exhibit ectopic expression of canonical eye development factors. (**A**) Confocal images of sections through endogenous (i,iii,v,vii,ix) and ectopic (ii,iv,vi,viii,x) eyes immunostained for the retinal differentiation markers Glutamine synthetase (Muller cells, red), Islet-1 (amacrine cells, cyan), XAP2 (rods, yellow) and Calbindin (cones, green) and representative phase contrast images show similar differentiated retinal cell populations in endogenous and ectopic eyes. (**B**) Confocal images of sections through endogenous (i) and ectopic (ii) eyes co-immunostained for retinal cell differentiation markers of rods (yellow), Muller cells (magenta) and amacrine cells (cyan) and for nuclei (blue) show a similar organization of differentiated retinal cell populations. (**C**) In situ hybridization of stage 30 control embryos (i,iii,v) and embryos microinjected with DNKir6.1p mRNA (ii,iv,vi) in all four cells at the four-cell stage for eye development markers *Otx2* (i,ii), *Pax6* (iii,iv) and *Rx1* (v,vi). Red arrowheads mark ectopic expression, and green arrowheads mark endogenous expression. No ectopic *Otx2* expression is observed in the injected embryos.

that the V_{mem} signal functions in defining the pattern of these canonical EFTFs. Analysis of the timing of the bilateral hyperpolarization signal, the bilateral regionalization of *Rx1*/*Pax6* expression to eye domains, and the ability of dominant-negative *Pax6* to disturb the normal hyperpolarization pattern, all suggest a feedback loop between the biophysical and transcriptional signals. Cross-talk between *Pax6* and the V_{mem} signal might result in a dynamic bilateral regionalization of the eye field, similar to the role of progressive depolarization in the differentiation of human mesenchymal stem cells (Sundelacruz et al., 2009).

Consistent with the hyperpolarization-induced expression of eye genes such as *Pax6* and *Rx1*, eye tissue and indeed complete eyes can be formed by just one ion channel mRNA that modulates V_{mem}. Although often only patches of individual tissue (RPE or lens) are formed, complete whole eyes can be produced that have the tissue layers and anatomical structure of native eyes. The same phenotype resulted from induced flows of different ion species and could be manipulated by direct control of ionic gradients precisely as predicted by the Goldman equation. These data reveal that eye induction is mediated by changes in V_{mem} itself – a physiological parameter that is not necessarily tied to any one gene product,

Table 1. The V_{mem} eye induction signal is transduced via Ca^{2+} influx

Phenotype	Injected	Injected + Fluoxetine (10 μM)	Injected + Lindane (10 μM)	Injected + Verapamil (100 μM)
No ectopic eye tissue	55	36	33	42
Ectopic eye tissue	17	10	13	2
Total	72	46	46	44
Percentage ectopic eye tissue	23.6	21.7	28.2	4.5

much as substrate geometry is now known to be a physical parameter controlling cell behavior (Chen et al., 1998; Dike et al., 1999). This is a desirable property from the perspective of developing biomedical applications because interventions (e.g. small-molecule drug cocktails designed to control V_{mem} in key cell groups) are not dependent on any one protein but can take advantage of convenient channels or pumps expressed in the host.

Our data show that the bilateral hyperpolarizing V_{mem} signal in the anterior neural field plays a crucial role in regionalization of EFTF expression and thus eye development. Upon perturbation of the bilateral V_{mem} signal, a major proportion of the malformed eye phenotypes (74%) represent failure of eye field separation (e.g. eyes fused to brain, eyes fused along midline, and eyes with pigmented optic nerve/stalk). We propose a hypothetical model in

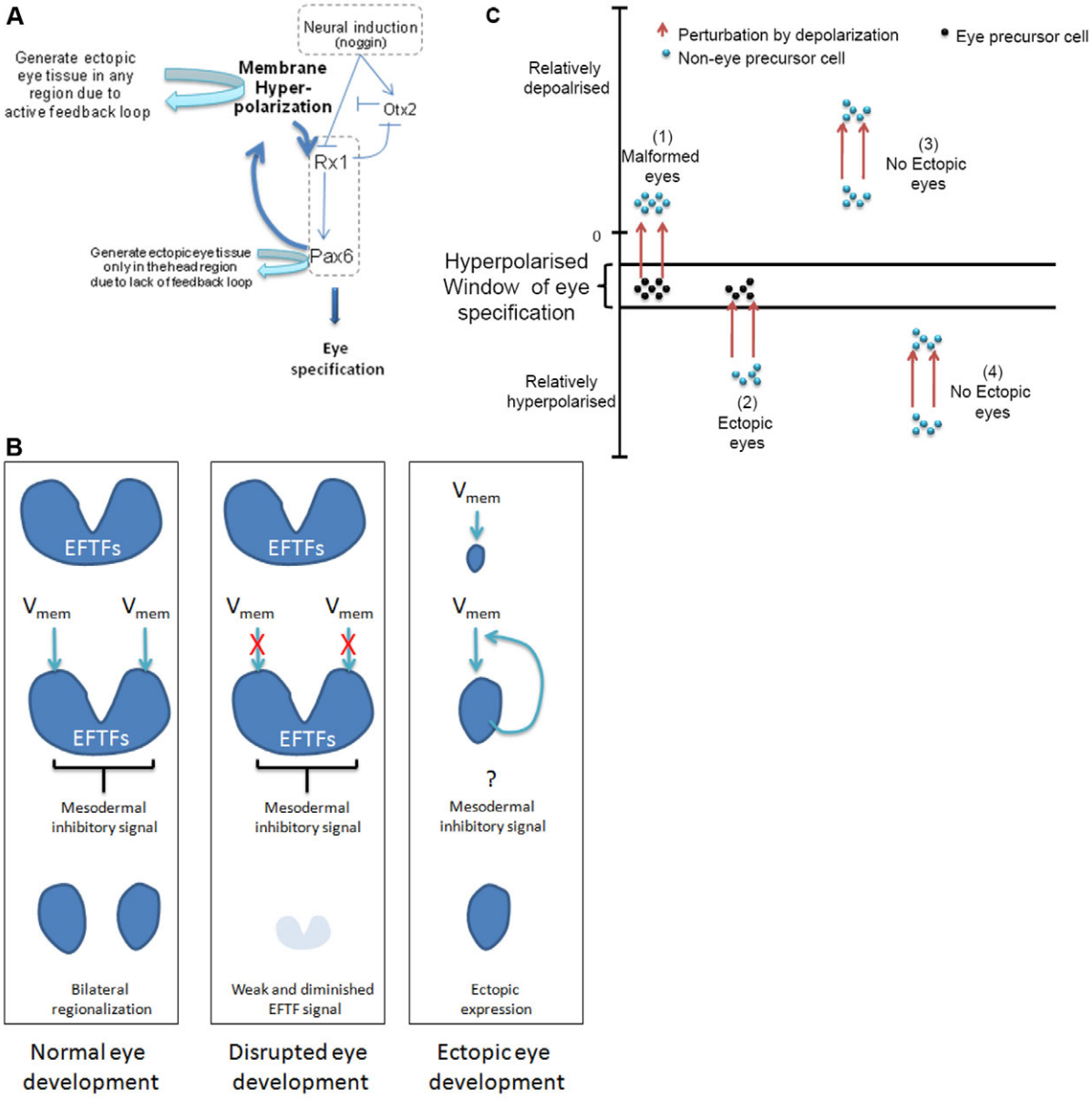

Fig. 5. Model integrating the V_{mem} signal into eye development and depicting the effects of its change on endogenous and ectopic eye development. (**A**) Neural induction is crucial in the process of eye development. Bilateral hyperpolarization of a cluster of cells in the anterior neural field regulates the expression pattern of eye development markers (EFTFs) such as *Rx1* and *Pax6*. Note that there is a positive-feedback loop between factors such as Pax6 and local hyperpolarization. (**B**) Eye development factor expression in relation to changes in V_{mem}. Normal eye development involves regulation of bilateral patterning of EFTFs by the bilateral V_{mem} signal (hyperpolarization). Underlying mesodermal inhibitory signal also plays an important role in this bilateral regionalization of EFTFs. Disruption of the bilateral V_{mem} signal results in diminished or lost EFTF signal, resulting in disrupted endogenous eye development. Induction of ectopic V_{mem} changes results in de novo EFTF expression and formation of ectopic eyes. (**C**) Hyperpolarization within a window of V_{mem} is important for the proper formation and development of eyes. Perturbation (depolarization, 1) of endogenous V_{mem} signal takes the cells outside this window and results in improper eye development. Perturbation (depolarization, 2) of V_{mem} of non-eye cells, such that their V_{mem} now lies within the window of eye formation, results in the formation of ectopic eye tissue by these cells. Perturbation (depolarization, 3 and 4) of V_{mem} in non-eye cells, such that their V_{mem} still does not fall within the eye formation window, does not result in ectopic eye tissue formation from these cells.

which feedback between V_{mem} and *Pax6* establishes a stable, bilaterally regionalized pattern of *Pax6* and other EFTF expression (Fig. 5A). Conversely, induction of an appropriate V_{mem} signal in non-eye cells results in ectopic induction and maintenance of EFTFs, driving the formation of ectopic eye tissues, perhaps by establishing the same stable feedback loop.

Neural tissue and *Otx2* expression are thought to be crucial for eye induction (Zuber et al., 2003). The ability to form ectopic eyes without induction of additional primary axes or central nervous system tissue (lack of ectopic *Otx2*) is very interesting and suggests a more direct (downstream) linkage of V_{mem} to eye-specific cascades (Fig. 5A). Indeed, bioelectrically induced eyes can be formed on the gut or within lateral mesoderm – non-neural tissues outside the known competence lineage for eyes. Similarly, patches of lens/retina readily form in the tail. By contrast, *Pax6* alone is incapable of initiating an eye field in regions outside the competent neurectoderm, suggesting that additional factors might also be involved in positive-feedback interactions with V_{mem}. However, V_{mem} is able to initiate not only *Pax6* expression but also the conditions that make tissues competent to form eyes upon *Pax6* transcription.

Temporally and spatially restricted hyperpolarization has previously been shown to drive cellular fate (Hinard et al., 2008; Konig et al., 2004; Konig et al., 2006; Sundelacruz et al., 2009). Moreover, specific cellular responses to windows of V_{mem} have also been documented (Gruler and Nuccitelli, 1991; Jurkat-Rott et al., 2009; McDonald et al., 1972). Our data suggest the presence of a narrow hyperpolarization range that specifies the V_{mem} signal for eye induction (Fig. 5C). Cells that are normally more strongly hyperpolarized than the eye-specific V_{mem} values can be driven into this range by depolarizing channels, whereas cells that are normally depolarized will be pushed into this range by hyperpolarizing channels. Accordingly, both depolarizing (dominant-negative K_{ATP}) and hyperpolarizing (Kv1.5) channels are capable of inducing ectopic eyes. The consequences of changes in V_{mem} (by altering $[Na^+]_{ex}$) in *Nav1.5*-injected embryos also support the induction of ectopic eye tissues when cells are moved into a narrow range of V_{mem}. Together, these data suggest a specific range of V_{mem} values for eye induction – changes in V_{mem} to levels above or below this target range do not result in eye induction. Also in line with this model, depolarization of endogenous eye field cells represses or disrupts eye formation by driving the V_{mem} of these cells out of the 'normal' permissive range. The narrow range of eye-compatible V_{mem} values is in line with our observation that only a small subset of injected cells within any tadpole form ectopic eye tissues.

In conclusion, we have characterized a V_{mem}-mediated signal that is necessary for patterning of *Pax6* and *Rx1* expression during normal eye development. This V_{mem} signal is also sufficient for induction of ectopic EFTF expression and eye formation. V_{mem}-induced ectopic eyes are formed in regions far outside the anterior neural tissues, which were conventionally thought to be the only region competent to form eyes. The discovery of bioelectrical signals that initiate the development of an organ as complex as the eye paves the way to important future work on the developmental and evolutionary roles of ion channel- and pump-derived gradients as mediators of patterning during embryogenesis. Moreover, the ability of changes in V_{mem} to initiate the formation of a complete vertebrate organ suggests a potential class of novel strategies for regenerative medicine and repair of birth defects (Levin, 2009).

Acknowledgements

We thank Punita Koustubhan, Amber Currier and Claire Stevenson for *Xenopus* husbandry and general laboratory assistance; Daryl Davies and Miriam Fine for the GlyCl expression construct; Franz Oswald for EosFP, Sally Moody for *Xenopus* Shh and Manuel Kukuljan for Nav1.5 constructs; Ali Hemmati-Brivanlou for DNPax6 and the *Pax6* antisense probe; Florian Lang for Kv1.5 plasmid; Erik Jorgensen for EXP1 plasmid; Michael Zuber for *Rx1* antisense probe; Valerie Schneider for *Otx2* antisense probe; and Dany S. Adams and Brook Chernet for microscopy assistance. The XAP2 and anti-Islet-1 antibodies developed by D. S. Sakaguchi and W. A. Harris and by T. M. Jessell and S. Brenner-Morton, respectively, were obtained from the Developmental Studies Hybridoma Bank (DSHB) developed under the auspices of the NICHD and maintained by The University of Iowa, Department of Biology, Iowa City, IA 52242, USA.

Funding

This work was supported by the National Institutes of Health (NIH) [EY018168 to M.L.]. S.A. was funded by the Agency for Science, Technology and Research (Singapore). M.L. is also grateful for the support of the G. Harold and Leila Y. Mathers Charitable Foundation. Deposited in PMC for release after 12 months.

Competing interests statement

The authors declare no competing financial interests.

Supplementary material

Supplementary material available online at
http://dev.biologists.org/lookup/suppl/doi:10.1242/dev.073759/-/DC1

References

Acampora, D., Mazan, S., Lallemand, Y., Avantaggiato, V., Maury, M., Simeone, A. and Brulet, P. (1995). Forebrain and midbrain regions are deleted in Otx2–/– mutants due to a defective anterior neuroectoderm specification during gastrulation. *Development* **121**, 3279-3290.

Adams, D. S., Masi, A. and Levin, M. (2007). H^+ pump-dependent changes in membrane voltage are an early mechanism necessary and sufficient to induce *Xenopus* tail regeneration. *Development* **134**, 1323-1335.

Andreazzoli, M., Gestri, G., Angeloni, D., Menna, E. and Barsacchi, G. (1999). Role of Xrx1 in Xenopus eye and anterior brain development. *Development* **126**, 2451-2460.

Aw, S., Koster, J. C., Pearson, W., Nichols, C. G., Shi, N. Q., Carneiro, K. and Levin, M. (2010). The ATP-sensitive K(+)-channel (K(ATP)) controls early left-right patterning in Xenopus and chick embryos. *Dev. Biol.* **346**, 39-53.

Bailey, T. J., El-Hodiri, H., Zhang, L., Shah, R., Mathers, P. H. and Jamrich, M. (2004). Regulation of vertebrate eye development by Rx genes. *Int. J. Dev. Biol.* **48**, 761-770.

Beane, W. S., Morokuma, J., Adams, D. S. and Levin, M. (2011). A chemical genetics approach reveals H,K-ATPase-mediated membrane voltage is required for planarian head regeneration. *Chem. Biol.* **18**, 77-89.

Beg, A. A. and Jorgensen, E. M. (2003). EXP-1 is an excitatory GABA-gated cation channel. *Nat. Neurosci.* **6**, 1145-1152.

Blackiston, D., Adams, D. S., Lemire, J. M., Lobikin, M. and Levin, M. (2011). Transmembrane potential of GlyCl-expressing instructor cells induces a neoplastic-like conversion of melanocytes via a serotonergic pathway. *Dis. Model. Mech.* **4**, 67-85.

Bowes, J. B., Snyder, K. A., Segerdell, E., Jarabek, C. J., Azam, K., Zorn, A. M. and Vize, P. D. (2010). Xenbase: gene expression and improved integration. *Nucleic Acids Res.* **38**, D607-D612.

Chen, C. S., Mrksich, M., Huang, S., Whitesides, G. M. and Ingber, D. E. (1998). Micropatterned surfaces for control of cell shape, position and function. *Biotechnol. Prog.* **14**, 356-363.

Chow, R. L., Altmann, C. R., Lang, R. A. and Hemmati-Brivanlou, A. (1999). Pax6 induces ectopic eyes in a vertebrate. *Development* **126**, 4213-4222.

Davies, D. L., Trudell, J. R., Mihic, S. J., Crawford, D. K. and Alkana, R. L. (2003). Ethanol potentiation of glycine receptors expressed in *Xenopus* oocytes antagonized by increased atmospheric pressure. *Alcohol Clin. Exp. Res.* **27**, 743-755.

Dike, L. E., Chen, C. S., Mrksich, M., Tien, J., Whitesides, G. M. and Ingber, D. E. (1999). Geometric control of switching between growth, apoptosis, and differentiation during angiogenesis using micropatterned substrates. *In Vitro Cell. Dev. Biol. Anim.* **35**, 441-448.

Erclik, T., Hartenstein, V., McInnes, R. R. and Lipshitz, H. D. (2009). Eye evolution at high resolution: the neuron as a unit of homology. *Dev. Biol.* **332**, 70-79.

Ericson, J., Thor, S., Edlund, T., Jessell, T. M. and Yamada, T. (1992). Early stages of motor neuron differentiation revealed by expression of homeobox gene Islet-1. *Science* **256**, 1555-1560.

Faber, J. and Nieuwkoop, P. D. (1967). *Normal Table of* Xenopus Laevis *(Daudin); a Systematical and Chronological Survey of the Development from Fertilized Egg Till the End of Metamorphosis*. Amsterdam: North Holland.

Fakler, B., Bond, C. T., Adelman, J. P. and Ruppersberg, J. P. (1996). Heterooligomeric Assembly of inward-rectifier K^+ channels from subunits of different subfamilies: Kir2.1 (IRK1) and Kir4.1 (BIR10). *Pflugers Arch.* **433**, 77-83.

Ficker, E., Dennis, A. T., Obejero-Paz, C. A., Castaldo, P., Taglialatela, M. and Brown, A. M. (2000). Retention in the endoplasmic reticulum as a mechanism of dominant-negative current suppression in human long QT syndrome. *J. Mol. Cell. Cardiol.* **32**, 2327-2337.
Fukumoto, T., Kema, I. P. and Levin, M. (2005). Serotonin signaling is a very early step in patterning of the left-right axis in chick and frog embryos. *Curr. Biol.* **15**, 794-803.
Gargini, C., Terzibasi, E., Mazzoni, F. and Strettoi, E. (2007). Retinal Organization in the retinal degeneration 10 (rd10) mutant mouse: a morphological and ERG study. *J. Comp. Neurol.* **500**, 222-238.
Gehring, W. J. and Ikeo, K. (1999). Pax6, mastering eye morphogenesis and eye evolution. *Trends Genet.* **15**, 371-377.
Gillespie, J. I. (1983). The distribution of small ions during the early development of *Xenopus laevis* and *Ambystoma mexicanum* embryos. *J. Physiol.* **344**, 359-377.
Gruler, H. and Nuccitelli, R. (1991). Neural crest cell galvanotaxis: new data and a novel approach to the analysis of both galvanotaxis and chemotaxis. *Cell Motil. Cytoskeleton* **19**, 121-133.
Harland, R. M. (1991). In situ hybridization: an improved whole-mount method for *Xenopus* embryos. *Methods Cell Biol.* **36**, 685-695.
Harris, W. A. and Messersmith, S. L. (1992). Two cellular inductions involved in photoreceptor determination in the *Xenopus* retina. *Neuron* **9**, 357-372.
Hinard, V., Belin, D., Konig, S., Bader, C. R. and Bernheim, L. (2008). Initiation of human myoblast differentiation via dephosphorylation of Kir2.1 K^+ channels at tyrosine 242. *Development* **135**, 859-867.
Hirsch, N. and Harris, W. A. (1997). Xenopus Pax-6 and retinal development. *J. Neurobiol.* **32**, 45-61.
Hough, E., Beech, D. J. and Sivaprasadarao, A. (2000). Identification of molecular regions responsible for the membrane trafficking of Kir6.2. *Pflugers Arch.* **440**, 481-487.
Huang, S. and Ingber, D. E. (2006). A non-genetic basis for cancer progression and metastasis: self-organizing attractors in cell regulatory networks. *Breast Dis.* **26**, 27-54.
Ingber, D. E. (2006). Mechanical control of tissue morphogenesis during embryological development. *Int. J. Dev. Biol.* **50**, 255-266.
Jurkat-Rott, K., Weber, M. A., Fauler, M., Guo, X. H., Holzherr, B. D., Paczulla, A., Nordsborg, N., Joechle, W. and Lehmann-Horn, F. (2009). K^+-dependent paradoxical membrane depolarization and Na^+ overload, major and reversible contributors to weakness by ion channel leaks. *Proc. Natl. Acad. Sci. USA* **106**, 4036-4041.
Konig, S., Hinard, V., Arnaudeau, S., Holzer, N., Potter, G., Bader, C. R. and Bernheim, L. (2004). Membrane hyperpolarization triggers myogenin and myocyte enhancer factor-2 expression during human myoblast differentiation. *J. Biol. Chem.* **279**, 28187-28196.
Konig, S., Beguet, A., Bader, C. R. and Bernheim, L. (2006). The calcineurin pathway links hyperpolarization (Kir2.1)-induced Ca^{2+} signals to human myoblast differentiation and fusion. *Development* **133**, 3107-3114.
Kurtz, I. and Schrank, A. R. (1955). Bioelectric properties of intact and regenerating earthworms *Eisenia foetida*. *Physiol. Zool.* **28**, 322-330.
Levin, M. (2006). Is the early left-right axis like a plant, a kidney, or a neuron? The Integration of physiological signals in embryonic asymmetry. *Birth Defects Res. C Embryo Today* **78**, 191-223.
Levin, M. (2007). Large-scale biophysics: ion flows and regeneration. *Trends Cell Biol.* **17**, 261-270.
Levin, M. (2009). Bioelectric mechanisms in regeneration: unique aspects and future perspectives. *Semin. Cell Dev. Biol.* **20**, 543-556.
Levin, M., Thorlin, T., Robinson, K. R., Nogi, T. and Mercola, M. (2002). Asymmetries in H^+/K^+-ATPase and cell membrane potentials comprise a very early step in left-right patterning. *Cell* **111**, 77-89.
Lupo, G., Harris, W. A., Barsacchi, G. and Vignali, R. (2002). Induction and patterning of the telencephalon in *Xenopus laevis*. *Development* **129**, 5421-5436.
Marsh, G. and Beams, H. W. (1947). Orientation of growth direction of the onion root in a transverse electric field. *Anat. Rec.* **99**, 623.
McCaig, C. D., Song, B. and Rajnicek, A. M. (2009). Electrical dimensions in cell science. *J. Cell Sci.* **122**, 4267-4276.
McDonald, T. F., Sachs, H. G., Orr, C. W. and Ebert, J. D. (1972). External potassium and baby hamster kidney cells: intracellular ions, ATP, growth, DNA synthesis and membrane potential. *Dev. Biol.* **28**, 290-303.
Moody, S. A. (1987). Fates of the blastomeres of the 32-cell-stage *Xenopus* embryo. *Dev. Biol.* **122**, 300-319.
Morokuma, J., Blackiston, D., Adams, D. S., Seebohm, G., Trimmer, B. and Levin, M. (2008). Modulation of potassium channel function confers a hyperproliferative invasive phenotype on embryonic stem cells. *Proc. Natl. Acad. Sci. USA* **105**, 16608-16613.
Nakanishi, S. and Okazawa, M. (2006). Membrane potential-regulated Ca^{2+} signalling in development and maturation of mammalian cerebellar granule cells. *J. Physiol.* **575**, 389-395.
Nichols, C. G. (2006). KATP channels as molecular sensors of cellular metabolism. *Nature* **440**, 470-476.
Nishiyama, M., von Schimmelmann, M. J., Togashi, K., Findley, W. M. and Hong, K. (2008). Membrane potential shifts caused by diffusible guidance signals direct growth-cone turning. *Nat. Neurosci.* **11**, 762-771.
Onkal, R., Mattis, J. H., Fraser, S. P., Diss, J. K., Shao, D., Okuse, K. and Djamgoz, M. B. (2008). Alternative splicing of Nav1.5: an electrophysiological comparison of 'neonatal' and 'adult' isoforms and critical involvement of a lysine residue. *J. Cell. Physiol.* **216**, 716-726.
Pahuja, S. L., Mullins, B. T. and Reid, T. W. (1985). Bovine retinal glutamine synthetase 1. Purification, characterization and immunological properties. *Exp. Eye Res.* **40**, 61-74.
Pannese, M., Polo, C., Andreazzoli, M., Vignali, R., Kablar, B., Barsacchi, G. and Boncinelli, E. (1995). The Xenopus homologue of Otx2 is a maternal homeobox gene that demarcates and specifies anterior body regions. *Development* **121**, 707-720.
Prevarskaya, N., Skryma, R. and Shuba, Y. (2010). Ion channels and the hallmarks of cancer. *Trends Mol. Med.* **16**, 107-121.
Reid, B., Song, B., McCaig, C. D. and Zhao, M. (2005). Wound healing in rat cornea: the role of electric currents. *FASEB J.* **19**, 379-386.
Romero, M. F., Henry, D., Nelson, S., Harte, P. J., Dillon, A. K. and Sciortino, C. M. (2000). Cloning and characterization of a Na^+-driven anion exchanger (NDAE1). A new bicarbonate transporter. *J. Biol. Chem.* **275**, 24552-24559.
Schwappach, B., Zerangue, N., Jan, Y. N. and Jan, L. Y. (2000). Molecular basis for K(ATP) assembly: transmembrane interactions mediate association of a K^+ channel with an ABC transporter. *Neuron* **26**, 155-167.
Secchi, A. G., Segato, T. and Mancini, B. (1976). Release of protein and cations from the lens in the presence of different antigen-antibody interactions. *Mod. Probl. Ophthalmol.* **16**, 80-94.
Shan, Q., Haddrill, J. L. and Lynch, J. W. (2001). Ivermectin, an unconventional agonist of the glycine receptor chloride channel. *J. Biol. Chem.* **276**, 12556-12564.
Shi, R. and Borgens, R. B. (1995). Three-dimensional gradients of voltage during development of the nervous system as invisible coordinates for the establishment of embryonic pattern. *Dev. Dyn.* **202**, 101-114.
Sive, H., Grainger, R. M. and Harland, R.,. (2000). *Early Development of Xenopus Laevis: A Laboratory Manual*. New York: Cold Spring Harbor Laboratory Press.
Strutz-Seebohm, N., Gutcher, I., Decher, N., Steinmeyer, K., Lang, F. and Seebohm, G. (2007). Comparison of potent Kv1.5 potassium channel inhibitors reveals the molecular basis for blocking kinetics and binding mode. *Cell. Physiol. Biochem.* **20**, 791-800.
Sundelacruz, S., Levin, M. and Kaplan, D. L. (2009). Role of membrane potential in the regulation of cell proliferation and differentiation. *Stem Cell Rev.* **5**, 231-246.
Tseng, A. S., Beane, W. S., Lemire, J. M., Masi, A. and Levin, M. (2010). Induction of vertebrate regeneration by a transient sodium current. *J. Neurosci.* **30**, 13192-13200.
Vandenberg, L. N., Morrie, R. D. and Adams, D. S. (2011). V-ATPase-dependent ectodermal voltage and Ph regionalization are required for craniofacial morphogenesis. *Dev. Dyn.* **240**, 1889-1904.
Viczian, A. S., Solessio, E. C., Lyou, Y. and Zuber, M. E. (2009). Generation of functional eyes from pluripotent cells. *PLoS Biol.* **7**, e1000174.
Wacker, S. A., Oswald, F., Wiedenmann, J. and Knochel, W. (2007). A green to red photoconvertible protein as an analyzing tool for early vertebrate development. *Dev. Dyn.* **236**, 473-480.
Wang, E., Reid, B., Lois, N., Forrester, J. V., McCaig, C. D. and Zhao, M. (2005). Electrical inhibition of lens epithelial cell proliferation: an additional factor in secondary cataract? *FASEB J.* **19**, 842-844.
Wang, Z., Tristani-Firouzi, M., Xu, Q., Lin, M., Keating, M. T. and Sanguinetti, M. C. (1999). Functional effects of mutations in KvLQT1 that cause long QT syndrome. *J. Cardiovasc. Electrophysiol.* **10**, 817-826.
Wolff, C., Fuks, B. and Chatelain, P. (2003). Comparative study of membrane potential-sensitive fluorescent probes and their use in ion channel screening assays. *J. Biomol. Screen.* **8**, 533-543.
Woodruff, R. I. and Telfer, W. H. (1980). Electrophoresis of proteins in intercellular bridges. *Nature* **286**, 84-86.
Yao, L., Shanley, L., McCaig, C. and Zhao, M. (2008). Small applied electric fields guide migration of hippocampal neurons. *J. Cell. Physiol.* **216**, 527-535.
Yasuda, T. and Adams, D. J. (2010). Physiological roles of ion channels in adult neural stem cells and their progeny. *J. Neurochem.* **114**, 946-959.
Zaghloul, N. A., Yan, B. and Moody, S. A. (2005). Step-wise specification of retinal stem cells during normal embryogenesis. *Biol. Cell* **97**, 321-337.
Zhao, M., Song, B., Pu, J., Wada, T., Reid, B., Tai, G., Wang, F., Guo, A., Walczysko, P., Gu, Y. et al. (2006). Electrical signals control wound healing through phosphatidylinositol-3-OH kinase-gamma and PTEN. *Nature* **442**, 457-460.
Zuber, M. E. (2010). Eye field specification in *Xenopus Laevis*. *Curr. Top. Dev. Biol.* **93**, 29-60.
Zuber, M. E., Gestri, G., Viczian, A. S., Barsacchi, G. and Harris, W. A. (2003). Specification of the vertebrate eye by a network of eye field transcription factors. *Development* **130**, 5155-5167.

Table S1. Anatomical distance measurements of the hyperpolarized region location

	Stage 18 CC2 signal		Stage 21 CC2 signal		Stage 21 *Rx1* in situ signal	
	Distance from neural groove (μm)	Distance from cement gland (μm)	Distance from neural groove (μm)	Distance from cement gland (μm)	Distance from neural groove (μm)	Distance from cement gland (μm)
	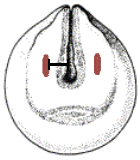	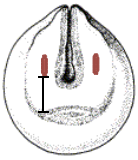	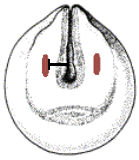	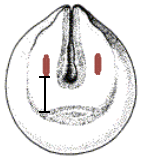	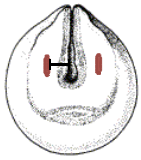	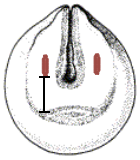
Embryo no.						
1	166	254	184	224	307	249
2	227	237	237	230	244	260
3	177	275	227	299	201	249
4	229	224	195	331	199	223
5	302	237	227	299	154	117
6	283	168	231	240	151	117
7	244	358	205	267	294	276
8	168	223	187		360	286
9	245	302	203			
10	245	213	235			
Average	228.6	249.1	213.1	270	238.8	221.9
s.d.	46.40	52.53	20.5	40.88	76.09	67.72

Two-way ANOVA analysis shows no statistical difference ($P>0.05$) in the lateral or anterior-posterior position of the hyperpolarized region (CC2 signal) between stage 18 and 21. Also, no statistical difference was found in the position of the stage 21 CC2 signal and *Rx1* in situ hybridization signal. See also Fig. 1. Illustrations reproduced with permission from Nieuwkoop and Faber (Nieuwkoop and Faber, 1967).

Table S2. Ion channels that induce ectopic eye tissue in *Xenopus*

Injected channels	Percentage ectopic eye tissue phenotype	References
DNKir6.1pore	34	Aw et al., 2010
DNKir6.1-ER retention	26	Aw et al., 2010
DNKir6.1R185Q	16	Aw et al., 2010
DNSUR2ApEW10	16	Aw et al., 2010
DNKvLQT-V244M	30	Wang et al., 1999
Bir10-ER retention	13	Fakler et al., 1996
Kv1.5	19	Strutz-Seebohm et al., 2007
Neonatal NaV1.5	10	Onkal et al., 2008
666 (chimera mouse Kir6.2 fused to C-terminus of Kir2.1)	30	Hough et al., 2000
rKNBC (Na^+/HCO_3) transporter	11	Romero et al., 2000

See also Fig. 3.